

Highway roadside landslide stability analysis and management research

Zhiqiang Chen^{1, a}

¹ Northwest Research Institute Co.,Ltd of C.R.E.C, China

^a 2320610908@qq.com

Abstract. In order to manage the landslide on the side of a highway, the main sliding surface of the slope was determined by combining the monitoring data; and the finite element model was constructed to analyze the stress field and displacement field of the slope, and it was determined that the stability coefficient of the slope before the reinforcement did not satisfy the requirements of the engineering specification, and it was in the state of understability; the reinforcement scheme of "double-row skid-resistant piles + intercepting and draining Based on the analysis results and experts' opinions, the "double-row anti-slip pile + cut-off drainage" reinforcement scheme is formulated, and numerical analysis is used to analyze the stress and displacement changes of the reinforced slope and anti-slip pile, which verifies the feasibility of the reinforcement scheme. The research results show that: (1) the stability coefficient of the main slip surface of the slope before reinforcement is 0.913, which does not meet the requirements of engineering specifications. (2) The plastic deformation around the anti-slip pile after reinforcement is obviously reduced relative to that before reinforcement, indicating that the reinforcement scheme is effective. (3) The stability coefficient of the main section after reinforcement is improved by 30% relative to that before reinforcement, indicating that the reinforcement scheme is feasible.

Keywords: monitoring; sliding pile; strength reduction; stability

1. Introduction

Slope stability analysis has always been a hot issue in the field of geotechnical engineering, and experts and scholars have carried out a lot of research [1-4]. ZHONG Junhao et al [5] and others proposed a three-dimensional stability analysis method for local and overall instability of anti-slip pile-reinforced slopes under seismic force based on the upper limit theorem of limit analysis; ZHANG Bangxin et al [6] studied the reinforcement effect of different reinforcement schemes based on the comparison of the parameter sensitivity analysis of the soil and rock bodies; JIA Jianqing et al [7] verified the feasibility of the proposed method for the study of strength zoned anisotropy of soil bodies; LIU Zhongshuai et al [8] investigated the reinforcement effect of different reinforcement schemes; FENG Zhen et al [9] proposed the h-type anti-slip pile optimization method for slope stability based on different slope morphologies; TAO Lianjin et al [10] derived the displacement equation of anti-slip piles based on the limit analysis method, and compared the differences in the effects of far-field and near-field seismic waves on the stability of the slopes based on the susceptibility framework.

Anti-slip pile, as one of the commonly used technical means for slope reinforcement and management, plays an important role in preventing slope sliding damage and guaranteeing slope stability. In this paper, based on the stability analysis of a risky slope, combined with the expert opinion and the change of stress field and displacement field before reinforcement, the reinforcement and management scheme of double-row anti-slip piles is formulated, and the feasibility of the reinforcement scheme is verified by comparing and analyzing the change of stress field, displacement field and stability coefficient before and after reinforcement.

2. Project Overview

Slope project area is located in Guangdong Province, for a highway roadside slope. Is a southern subtropical monsoon climate, annual rainfall of 1300 ~ 1800mm, no surface water flow through the

area. The geomorphology of the project area is a low mountainous terrain, erosion cutting is relatively strong, the gully is not open, the top of the hills are mostly rounded, the topography of the ups and downs. The terrain is generally high in the south and low in the north, with an elevation of 250m~480m. The slope is relatively straight, with a slope gradient of 15~30°. The slope length is 817m, the roadbed width is 26m, the maximum excavation height is 70m, and the slope is divided into 7 levels. The bedrock in the project area is strongly weathered, with obvious differential weathering. Under the influence of excavation, the slope body has sliding deformation along the weak layer inside the rock body.

Due to the overall scale of the slope, it is affected by rainfall and construction disturbance, resulting in a serious threat to the operational safety of the highway at the foot of the slope. In order to ensure the safety of the slope, the slope was divided into 4 monitoring sections, 1-1, 2-2, 3-3 and 4-4, as shown in Fig. 1, to grasp the trend of slope stability change in real time through stress and displacement monitoring. The previous data show that the monitoring data of section 3-3 is unstable and has a high frequency of jumping, indicating that there is a great risk of sliding in this section. In view of this, section 3-3 is identified as the main sliding surface of the slope.

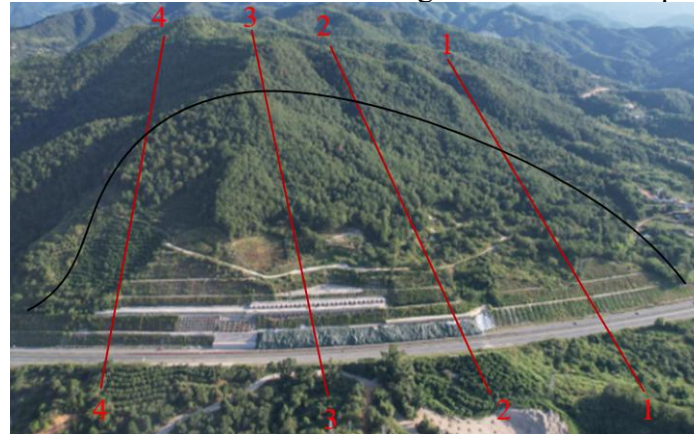


Fig. 1 Section Layout

3. Model Construction

According to the site investigation and borehole sampling, the stratigraphy from top to bottom mainly consists of: Quaternary Holocene Residual Slope Deposits, gravelly silty clay, Triassic Upper Xiaoping Formation Mudstone, Muddy siltstone and sandstone strata. The geological structure is shown in Fig. 2, and the physical and mechanical parameters of the geotechnical body are shown in Table 1.

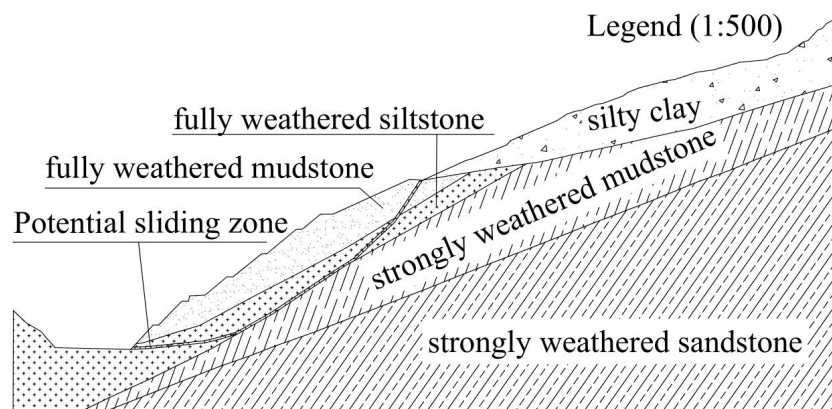


Fig. 2 Geological Tectonics

Table 1. Physical and mechanical parameters

Category	Severe/(kN.m ⁻³)	Cohesion/kPa	Friction angle/(°)	Modulus of elasticity/MPa	Poisson's ratio
----------	------------------------------	--------------	--------------------	---------------------------	-----------------

sliding belt	18	21.5	16	14	0.3
powdery clay	20	23	16.4	15	0.35
fully weathered mudstone	19	12	20	200	0.32
fully weathered sandstone	21.5	13.5	22	240	0.3
strongly weathered mudstone	22	24	25	300	0.37
strongly weathered sandstone	23.3	27	26.5	320	0.34
Pile	24	-	-	30000	0.2

Based on Moore-Cullen theory and finite element theory, a finite element model is constructed for the 3-3 section as shown in Figure 3. Horizontal and vertical displacement constraints are imposed on the bottom surface of the model, horizontal displacement constraints are imposed on both sides, and the model is meshed with plane strain (CPE4) cell type.



Fig. 3 Finite element model

4. Stability Analysis

The intersection point of the slope and the 7-level platform was selected as the tracking research point, and the inflection point of the displacement curve was taken as the judgment standard of slope instability, and the stress field and displacement field were analyzed on the main slip surface, and the stress cloud and displacement cloud were obtained as shown in Fig. 4 and Fig. 5, respectively.

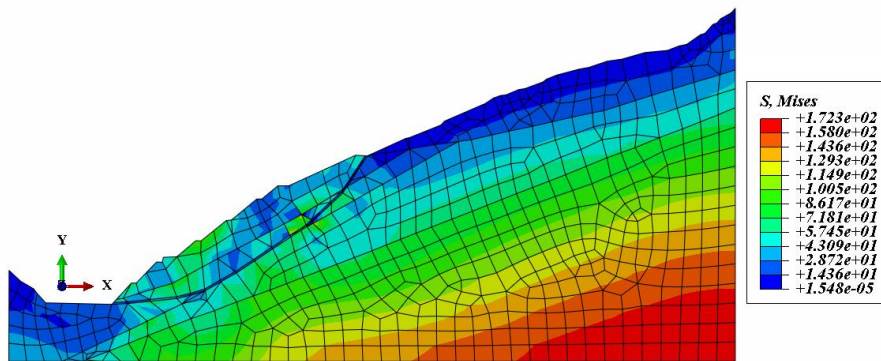


Fig. 4 Stress cloud diagram

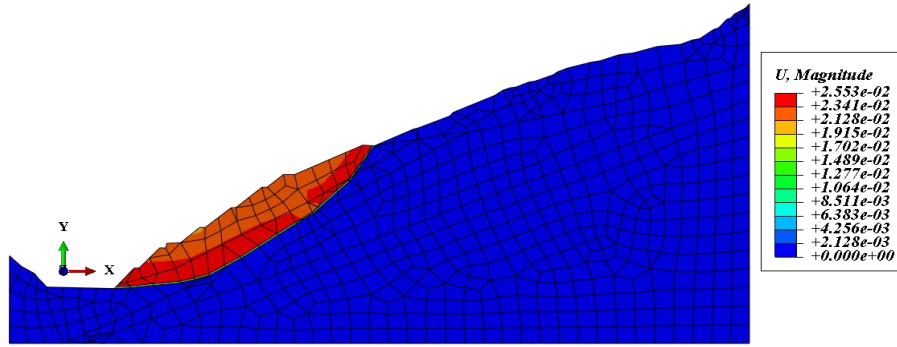


Fig. 5 Displacement cloud map

As can be seen in Figures 4 and 5, the average stress distribution gradually increases from top to bottom, and is obviously stratified according to the distribution locations of silty clay, fully weathered mudstone, fully weathered sandstone, strongly weathered mudstone, strongly weathered sandstone, and the average stress inside the strongly weathered sandstone at the bottom reaches a maximum of 172.3 kPa, the overall average stress in the upper part of the slope surface is on the small side, and the average stress in the area above the potential sliding zone is on the large side; the slope displacement is mainly concentrated in the sliding zone and the distribution area above it, and the maximum displacement value is 25.53 mm, and the rest of the area is relatively stable.

The strength of the geotechnical body was discounted, and the change in displacement at the tracking point was analyzed to obtain the change curve of the stability coefficient of the main section as shown in Fig. 6.

As can be seen from Figure 6: the stability coefficient of the main section is 0.913, while the engineering specification standard stipulates that the stability coefficient of this kind of slope in natural working condition ranges from 1.2 to 1.3, indicating that the section does not meet the stability requirements, and is in the state of instability. Affected by the rainfall and construction disturbance, the stability coefficient will continue to decline, and it is urgent to take targeted measures for slope stabilization and management.

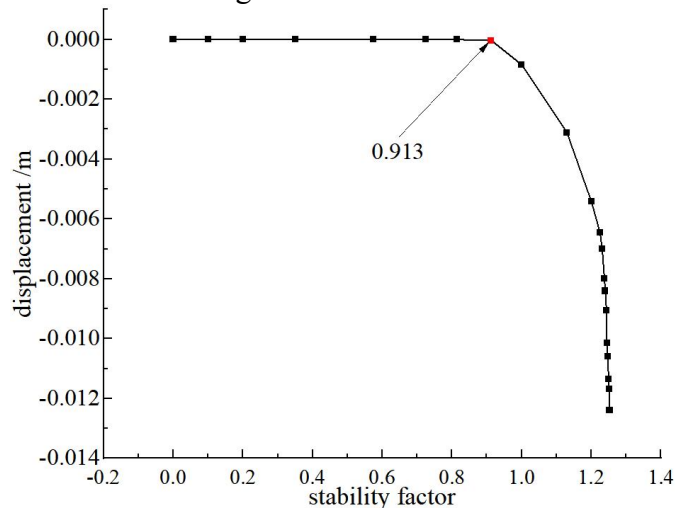


Fig. 6 Stability coefficient variation curve

5. Governance analysis

Combined with the results of stability analysis of the main section and expert discussion, it is determined to adopt "anti-slip piles + intercepting and draining" reinforcement program for slope management. The first row of anti-slip piles is laid in the middle of potential sliding zone, adopting square anti-slip piles with cross-section of 1.5m×2m, pile length of 9m, embedded in the inner 7.5m of the slope, exposed 1.5m on the slope surface, and pile spacing of 2m; the second row of anti-slip piles is laid in the foot of the slope, adopting square anti-slip piles with cross-section of 1.5m×2m,

pile length of 7m, embedded 6m in the inner 6m of the slope, exposed 1m on the slope surface, and pile spacing of 2m; and a rectangular intercepting gutter is added at the top of the slope, adopting slurry masonry sheet, with the use of slurry masonry sheet and drainage. The top of the slope is added with rectangular interceptor ditch, which is constructed with slurry masonry schist, and the specific layout is shown in Fig. 7.

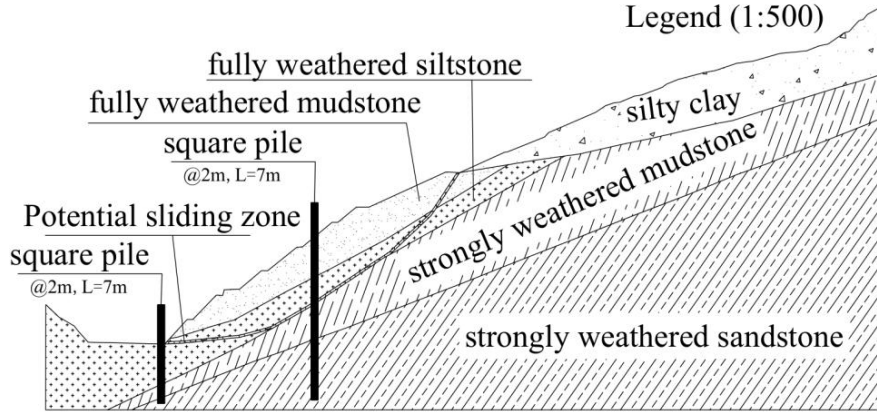


Fig. 7 Reinforcement Program

The finite element model is constructed according to the reinforcement scheme as shown in Fig. 8, horizontal and vertical displacement constraints are applied to the bottom surface of the model, horizontal displacement constraints are applied to both sides, and the slope is meshed with plane strain (CPE4) cell type and the anti-slip pile is meshed with beam (B21) cell type.



Fig. 8 Finite element model

Stress field and displacement field analyses were carried out on the reinforced slope to verify the feasibility of the reinforcement scheme, and the stress and displacement clouds of the reinforced slope as a whole were obtained as shown in Fig. 9 and Fig. 10, respectively, and those of the anti-slip pile were shown in Fig. 11.

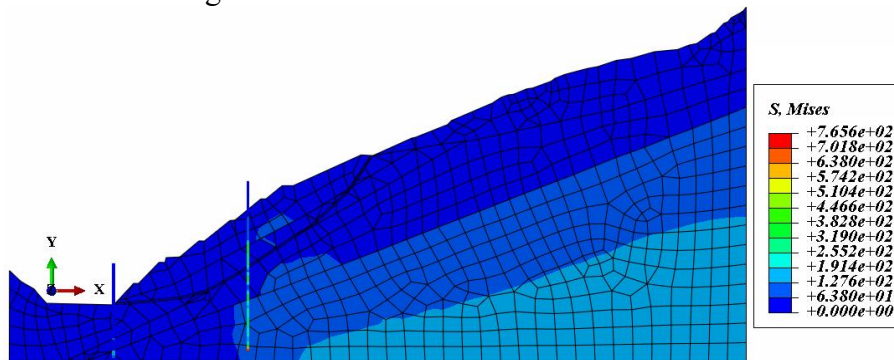


Fig. 9 Stress cloud of the slope

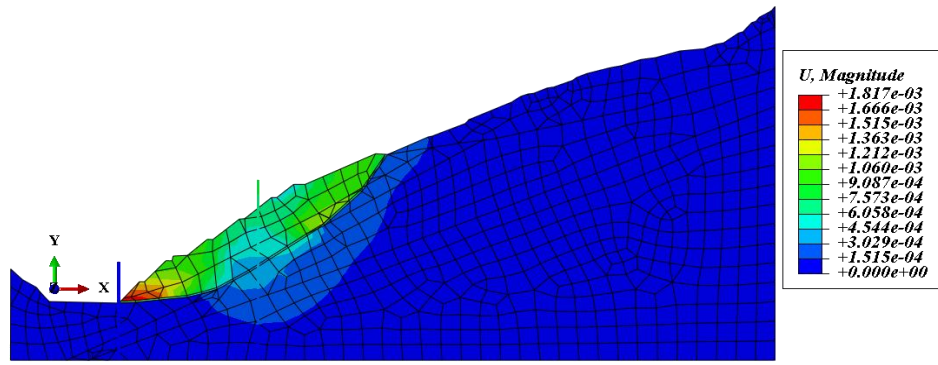


Fig. 10 Cloud map of slope displacement

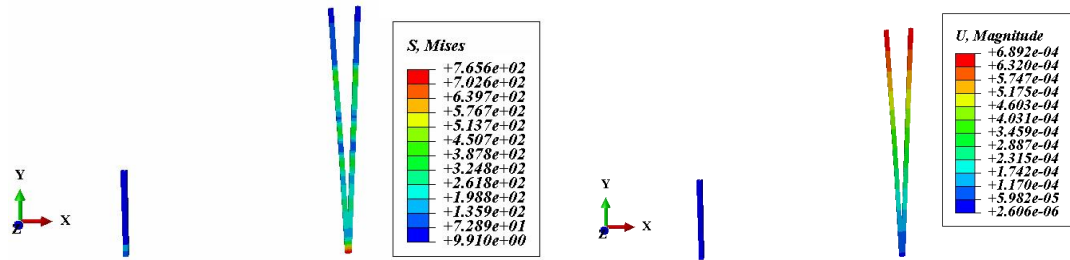


Fig. 11 Stress and displacement cloud of anti-slip pile

It can be seen from Fig. 9 and Fig. 10: the average stress of the slope body decreased by 25.9% after reinforcement, which is similar to the distribution characteristics before reinforcement, i.e., it gradually increased from the slope surface to the inside of the slope body, and the maximum average stress was 127.6kPa; the sliding area of the slope body after reinforcement is still concentrated in the sliding zone and the distribution position of the fully weathered mudstone above it, and the maximum displacement was 1.817mm, which was reduced by 92.9% compared with the pre-strengthening, and the plastic deformation around the sliding zone is relatively high, indicating that the anti-slip pile has an important effect on preventing the rock and soil body from sliding. And the plastic deformation around the sliding zone is relatively smaller than the two ends of the sliding zone, indicating that the anti-slip piles play an important role in preventing the sliding damage of the geotechnical body. From Fig. 11, it can be seen that the deformation of anti-slip piles at the top of the slope is obviously larger than that at the bottom; the displacement and deformation of both types of anti-slip piles are small, and there is no shear deformation, which indicates that the resistance produced by anti-slip piles is larger than the sliding force of the slope.

The strength of the reinforced slope geotechnical body is discounted, and the tracking points consistent with the pre-strengthening are selected for stability analysis, and the change of the stability coefficient of the reinforced slope is obtained as shown in Fig. 12.

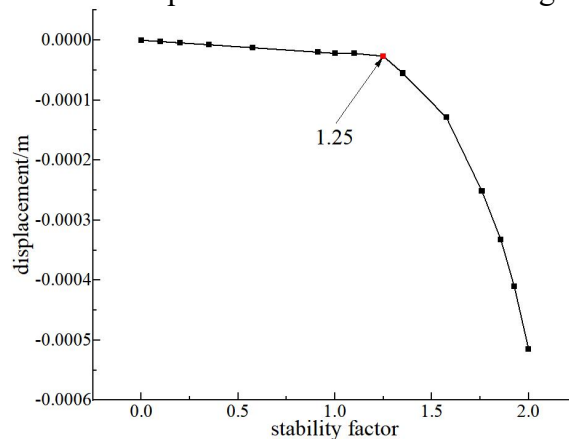


Fig. 12 Curve of variation of stability coefficient after reinforcement

As can be seen from Figure 12: the stability coefficient of this section after reinforcement is 1.25, which is 30% higher relative to the pre-strengthening period, satisfying the reinforcement requirements in the specification and indicating that the reinforcement scheme is feasible.

6. Conclusion

(1) The stability coefficient of the main slip face of the slope before reinforcement is 0.913, which does not meet the requirements of engineering specifications, indicating that the section is in an unstable state.

(2) The stress field and displacement field of the main section of the slope after reinforcement are obviously reduced relative to that before reinforcement, and the plastic deformation around the anti-slip pile is obviously reduced, which indicates that the reinforcement program has produced effective reinforcement effect.

(3) The stability coefficient of the reinforced slope is 1.25, which is 30% higher than that before reinforcement, and meets the requirements of engineering specifications, indicating that the reinforcement program is feasible.

Acknowledgments

This work was financially supported by National Key R&D Project (2022YFC3002603), Chongqing Natural Science Foundation Upper-level Project (CSTB2023NSCQ-MSX0878), Major Science and Technology Special Project/Key R&D Task Special Project of the Autonomous Region (2022B03033-2)

References

- [1] ZHANG Bangxin, JIA Jianqing, LAI Yuanming, et al. Study on slope stability considering zonal anisotropy and seepage. *Journal of Civil and Environmental Engineering (in English and Chinese)*, 2023, 45(4): 41-48.
- [2] ZHANG Zewei, LIU Sujia, ZHANG Ga. Centrifugal modeling experimental study of anti-slip pile-anchor reinforcement of slopes under precipitation conditions. *Journal of Geotechnical Engineering*, 2023, 45(S1): 206-209.
- [3] ZENG Yalin, JIN Bo, WANG Qishun, et al. Stability analysis of high-fill slope reinforced by anti-slip pile-reinforced soil combination based on limit theory. *Journal of Railway Science and Engineering*, 2023, 20(9): 3362-3372.
- [4] ZHANG Wengang, WANG Qi, CHEN Fuyong, et al. Study on slope reliability analysis and random response of anti-slip pile considering spatial variability of rock mass. *Geotechnics*, 2021, 42(11): 3157-3168.
- [5] ZHONG Junhao, YANG Xiaoli . Three-dimensional stability analysis of skid pile reinforced slopes under localized instability conditions. *China Safety Production Science and Technology*, 2023, 19(8): 108-115.
- [6] ZHANG Bangxin, JIA Jianqing, LIU Zhongshuai, et al. Stability analysis of Xiafen slope and its management measures. *Journal of Lanzhou Jiaotong University*, 2023, 42(1): 9-15.
- [7] JIA Jianqing, ZHANG Bangxin, TIAN Ming, et al. Study on the effect of anisotropy of soil strength zoning on slope stability. *Journal of Natural Hazards*, 2023, 32(1): 76-83.
- [8] LIU Zhongshuai, ZHANG Bangxin, YAN Zongling ,et al. Research on real-time monitoring and optimization of stabilization scheme of G220 landslide in Jinggangshan. *China Safety Production Science and Technology*, 2022, 18(S1): 42-47.
- [9] FENG Zhen, WANG Boyi, LIU Haoran, et al. Analysis of reinforcement effect of h-type anti-slip pile based on slope morphology. *Science Technology and Engineering*, 2022, 22(30): 13467-13476.
- [10] TAO Lianjin, WEN Hu, JIA Zhibo, et al. Research on performance-based design method of combined slope stabilization. *Journal of Engineering Geology*, 2022, 30(5): 1620-1628.